

Improved Variogram Models for More Realistic Estimation and Simulation

Michael J. Pyrcz¹ and Clayton V. Deutsch²

Geostatistical models often require a variogram or covariance model for kriging and kriging-based simulation. Next to the initial decision of stationarity, the choice of an appropriate variogram model is the most important decision in a geostatistical study. Common practice consists of fitting experimental variograms with a nested combination of proven models such as the spherical, exponential, and Gaussian models. These models work well in most cases; however, there are some “shapes” found in practice that are difficult to fit. Greater flexibility is available through the application of geometric and spectral corrected variogram models.

We introduce a family of variogram models that are based on geometric shapes, analogous to the spherical variogram, that are known to be positive definite and that provide additional flexibility to fit variograms encountered in practice. The positive definiteness of these models is established.

Fitting variograms with analytical models can be tedious and restrictive. There are many smooth functions that could be used for the variogram; however, arbitrary interpolation of the variogram will almost certainly create an invalid non-positive definite function. The idea of spectral correction, that is, taking the Fourier transform of the corresponding covariance values, resetting all negative terms to zero, standardizing the spectrum to sum to the sill, and inverse transforming the result has been proposed by numerous authors. This paper addresses some important implementation details.

Keywords: covariance, nested structures, kriging, stochastic simulation, Fourier transform

Introduction

There have been recent developments in the application of multipoint statistics. These methods will ultimately complement the more humble two-point variogram calculated from actual data. While these methodologies have potential, practical geostatistics continues to be driven by the variogram, because of (1) a lack of demonstrated case studies and procedures with multiple point statistics and (2) in many cases the variogram represents the limit of statistics that may be reliably extracted from the available data. Multiple point statistics beyond the variogram may require an assumption of stationarity with respect to a training image. This decision may be questionable if the training image over constrains the space of uncertainty or imparts artifacts non-representative features

¹ Department of Civil and Environmental Engineering, University of Alberta, Edmonton, AB, Canada
e-mail: mpyrcz@ualberta.ca

² Department of Civil and Environmental Engineering, University of Alberta, Edmonton, AB, Canada
e-mail: cdeutsch@ualberta.ca

from the training image. For these reasons, the variogram will remain significant into the foreseeable future.

The random function paradigm of geostatistics involves three main steps: **(1)** definition of the variable and the stationary domain for the variable $\{Z(\mathbf{u}), \mathbf{u} \in A\}$, which involves the definition of rock types/facies and large scale trends, **(2)** establish a variogram model for the variable, $\gamma(\mathbf{h})$, that is valid for all distances and directions found in the domain A , and **(3)** make inferences with kriging and Monte Carlo simulation. The reasonableness of the inferences depends on the first two steps. The expert site-specific decision of a stationary domain is arguably the most important; however, the calculation and fitting of a variogram model is also very important. The inference step is largely automatic once the first two steps are taken. This paper is aimed at the second step of establishing a valid variogram model. The conventional method of modeling variograms by nested structures is reviewed. While this method guarantees a variogram model that is positive definite in all directions, it may be viewed as restrictive. A suite of geometric variograms is introduced and the procedures required to apply spectral corrected fitted variogram models is outlined. These alternative methods allow for greater flexibility in the generation of permissible variogram models.

Conventional Variogram Modeling

The variogram of traditional geostatistics characterizes heterogeneity or predictability of the variable under consideration. Variogram models must be positive definite. This property ensures that the variogram is an appropriate measure of distance and that all resulting variances will be non-negative for all possible configurations of conditioning data (Journel and Huijbregts, 1978, p. 35).

Experimental variogram points are calculated in the principal directions allowing for some distance and direction tolerance to find sufficient pairs. The experimental points are fitted with a sum of nested structures.

$$\gamma(\mathbf{h}) = \sum_{i=0}^{nst} C_i \Gamma_i(\mathbf{h}) \quad (1)$$

where nst is the number of nested structures, $i = 0$ is commonly reserved for the nugget effect, and $\Gamma_i(\mathbf{h})$ functions are valid variogram functions defined by a shape (spherical, exponential, etc.), rotation angles to allow \mathbf{h} to be represented in the principal directions of continuity $(\mathbf{h}_1, \mathbf{h}_2, \mathbf{h}_3)$, and range parameters to account for anisotropy. A geometric transformation is applied to convert the 3-D distance vector, \mathbf{h} , to a scalar distance h [Eq.(2)].

$$h = \sqrt{\left(\frac{\mathbf{h}_1}{a_1}\right)^2 + \left(\frac{\mathbf{h}_2}{a_2}\right)^2 + \left(\frac{\mathbf{h}_3}{a_3}\right)^2} \quad (2)$$

Variogram modeling has relied on fitting known positive definite functions such as spherical, exponential and Gaussian models. Some additional flexibility is available since linear combinations and products of positive definite covariance models are known to be positive definite (Deutsch and Journel, 1998, p. 24). While this provides a workable mechanism for modeling continuity, there are some cases that are not well fit with this framework (see Figure 1 for an example structure commonly observed in experimental variograms).

The application of more flexible variogram modeling is inhibited by the difficulty in ensuring positive definiteness. There is a largely unexplored suite of positive definite models known as *geometric variograms* that provides some additional flexibility. They are genetically guaranteed to be positive definite and therefore avoid the burden of proof required by arbitrary variogram functions.

Geometric Variograms

Any covariance model based on a moving average of a generalized Poisson process is positive definite (Matérn, 1960, p. 28). Geometric variograms result from the special case of averaging where the weighting function is reduced to a Dirac function of the form:

$$f(\mathbf{u}) = i_v(\mathbf{u}) = \begin{cases} 1, & \text{if } \mathbf{u} \in V \\ 0, & \text{if } \mathbf{u} \notin V \end{cases}$$

$$F(\mathbf{u}) = K_v(\mathbf{h}) = \int i_v(\mathbf{u}) \cdot i_v(\mathbf{u} + \mathbf{h}) d\mathbf{u} \quad (3)$$

$$\gamma(\mathbf{h}) = 1 - \frac{K_v(\mathbf{h})}{V}$$

This amounts to the volume of intersection $K_v(\mathbf{h})$ of any geometric object with itself offset by a lag vector, \mathbf{h} . Where $K_v(0)$, the volume of the geometric object, is analogous to the sill, $C(0)$, of the covariance model. The construction of a geometric variogram is illustrated in Figure 2. A positive definite model in n-D is valid in any less or equal dimensional space; for example the spherical variogram is valid in 3, 2 and 1 dimensions.

In some cases analytical equations may be available for the volumes of intersection. Numerical integration can always be used for complicated geometric objects. The volume of intersection could be efficiently calculated as:

$$K_v(\mathbf{h}_x, \mathbf{h}_y, \mathbf{h}_z) = \sum_{i_z}^{n_z} \sum_{i_y}^{n_y} \sum_{i_x}^{n_x} i(\mathbf{u}_x, \mathbf{u}_y, \mathbf{u}_z) \cdot i(\mathbf{u}_x + \mathbf{h}_x, \mathbf{u}_y + \mathbf{h}_y, \mathbf{u}_z + \mathbf{h}_z) \quad (4)$$

where $i(\mathbf{u}_x, \mathbf{u}_y, \mathbf{u}_z)$ and $i(\mathbf{u}_x + \mathbf{h}_x, \mathbf{u}_y + \mathbf{h}_y, \mathbf{u}_z + \mathbf{h}_z)$ are indicators set to 1 if within the object and 0 if without the object and $K_v(\mathbf{h}_x, \mathbf{h}_y, \mathbf{h}_z)$ is the volume of intersection given the lag vectors $\mathbf{h}_x, \mathbf{h}_y, \mathbf{h}_z$. The result is a discrete covariance model for kriging.

Isotropic Geometric Variogram Models

Isotropic geometric variogram models result from isotropic geometric objects. This is limited to lines (1-D), circles (2-D), spheres (3-D) and hyperspheres (n-D, $n > 3$). These geometric models account for anisotropy by scaling the component vectors [Eq. (2)].

Spherical Variogram

This variogram model is very commonly used. The spherical model is based on the standardized volume of intersection of two spheres separated by a lag vector (\mathbf{h}) as defined (Serra, 1967).

$$\gamma(\mathbf{h}) = 1 - \frac{\text{volume}(\mathbf{h})_{\text{int}}}{\text{volume}_{\text{total}}} \quad (5)$$

Analogous to the spherical variogram model in 3-D is the circular and triangular variogram models that are positive definite in 2-D and 1-D, respectively.

Hollowed Spherical Variograms

A variety of other isotropic geometric variogram models may be calculated by hollowing of the geometric object. For example the circle in 2-D may be changed to an annular region or the sphere to a hollowed sphere. The hollowed sphere results in a novel series of positive definite 3-D variogram models parameterized by the inner radius (r_1) or fraction of hollowing. A series of hollowed spherical variogram models are shown in Figure 3.

In the limiting cases this variogram is equivalent to the spherical model when r_1 equals 0.0 (the sphere is not hollowed) and approaches the nugget effect as $r_1 \rightarrow r_2$. The difference between the hollowed spherical variogram and the spherical variogram is equivalent to the volume of intersection lost due to the hollowed inner sphere (Figure 4). An example hollowed sphere (fraction hollowed 0.75) raster image and covariance table is shown in Figure 5.

Anisotropic Geometric Variogram Models

Any geometric shape in any dimension leads to a valid variogram model. Slices through an approximated shape of a point bar inclined heterolithic strata (IHS) are shown on the top of Figure 6. The covariance table was calculated for this object and is shown on the bottom of Figure 6. This complicated anisotropic geometric object has resulted in a complicated anisotropic covariance table.

There are a variety of geologic geometries that may be applied to calculate variogram models. For example, characteristic geometries of architectural elements from fluvial depositional settings such as lateral accretion, downstream accretion, channel fills etc. (Miall, 1999, p. 93) may be suitable.

There is a limit on the information that geometry may provide with respect to the variogram model. For example, the randomly positioned spheres result in the bombing variogram model not the spherical variogram model. Yet the geometry may provide information with respect to the general variogram shape and anisotropy. While the variogram can be tailored to the geometry of the underlying phenomenon, in the absence of insight into geometry of the underlying phenomenon, the determination of the appropriate geometric shape to fit a complicated variogram is an intractable inverse problem.

While the application of geometric variogram models may improve variogram modeling flexibility, greater flexibility is possible by application of spectral correction to fitted variogram models.

Spectral Corrected Variogram Models

Fitting an arbitrary function to experimental variogram points, $\gamma(\mathbf{h})$, will not lead to a valid positive definite model for subsequent estimation and simulation. Spectral correction offers an efficient means to correct arbitrary fitted variogram to be positive definite.

Positive Definiteness

We switch to the covariance, $C(\mathbf{h})$, that is related to the variogram when the underlying random function is second order stationary by:

$$C(\mathbf{h}) = C(0) - \gamma(\mathbf{h}) \tag{6}$$

The covariance is commonly used instead of the variogram to solve for kriging weights due to convenience in the matrix solution.

Positive definiteness, or more precisely non-negative definiteness, is a constraint that all possible variances must be non-negative. Given that the estimate is the result of a finite linear combination:

$$y^*(\mathbf{u}) = \sum_{i=1}^n \lambda_i z(\mathbf{u}_i) \quad (7)$$

This constraint may be expressed as:

$$\sigma_k^2\{\mathbf{u}\} = \sum_i \sum_j \lambda_i \lambda_j C(\mathbf{u}_i, \mathbf{u}_j) \geq 0 \quad (8)$$

where $\sigma_k^2(\mathbf{u})$ is the estimation variance that is minimized by the kriging equations. Also positive definiteness ensures that the all covariance matrices calculated with the covariance function will be positive definite. Proving this constraint [Eq. (8)] for a specific covariance model, $C(\mathbf{h})$, amounts to proving that all possible weights, resulting from all possible data settings, will result in non-negative variances. This procedure is not directly possible since all possible data configurations cannot be explored. The application of Bochner's theorem to remap a covariance model to a spectrum representation is required to correct for positive definiteness (Bochner, 1949).

Review of Spectral Methods

Bochner's theorem defines the general form of a positive definite function $C(\mathbf{h})$, continuous in $\mathbf{h} = 0$ (without nugget effect), as:

$$C(\mathbf{h}) = \int_{-\infty}^{\infty} \cos(\omega h) \cdot dS(\omega) \quad (9)$$

under the constraints that $dS(\omega) > 0$ and $\int_{-\infty}^{\infty} dS(\omega) = C(0) < \infty$. $S(\omega)$ is the spectral cumulative distribution function.

The practical result of the link between the spectrum and covariance models is an efficient method to check for positive definiteness and to correct for positive definiteness in discrete, tabulated, covariance models. A positive definite check of the spectrum representation amounts to checking if all real components are greater than 0.0 and that they sum to the variance ($C(0)$). A discrete covariance model is corrected by enforcing these constraints by setting all negative real components to 0.0 and then standardizing all spectrum to sum to the variance.

Proposed Flexible Variogram Modeling Procedure

A new methodology for flexible variogram modeling is proposed. This methodology requires the following steps: (1) model the variogram in the principal directions, (2)

construct a consistent covariance table from variograms in the principal directions and (3) correct these covariance tables for positive definiteness. The corrected covariance tables may be loaded directly into kriging or simulation.

Model the Variogram in the Principal Directions

These directional models may be regression fits of the experimental variogram points, or even hand drawn. The key is to build models that integrate geologic information.

Calculate a Consistent Covariance Table

From the arbitrary variogram models in the principal directions a consistent covariance table is inferred. The covariance table must have the same dimensionality and scale as the random function model to which it will be applied. The table is set large enough that the variogram to fully characterize the spatial continuity. Also, the size of the table is set to a power of 2 [Eq. (11)].

$$ncells_{x,y,z} = 2^{i_{x,y,z}} \quad (11)$$

where $i_{x,y,z}$ is an integer. This is required by the numerical recipes multidimensional discrete Fast Fourier Transform (FFT) subroutine (fourn.for) (Press, W.H. et. al., 1992, p. 499).

The traditionally applied linear model of regionalization requires that the variogram is inferred for directions other than the principals by applying geometric anisotropy [Eq. (2)] (Isaaks and Srivastava, 1989, p. 377). This method requires the directional variograms to be constructed from a common set of nested structures. Each nested structure must be effective over all directions. Since we have not applied a common set of nested structures, we require a new method to infer the variogram in the non-principal directions.

A new method of interpolating the variogram values in the off-diagonal directions is introduced based on variable geometric anisotropy. This method is limited by the assumptions (1) the variogram is provided in the principal directions and (2) the variogram models are monotonically increasing (no cyclicity or hole effect).

Variable geometric anisotropy is applied as follows: (1) the variogram model is binned by equal variance contributions, (2) the ranges in the principal directions are tabulated for each bin. These ranges parameterize nested ellipsoids that define the variogram in all directions with variable geometric anisotropy. These ellipsoids are demonstrated in Figure 8 and are represented by the following:

$$\left(\frac{h_x}{a_x(\gamma_x^{-1}(c^\ell))} \right)^2 + \left(\frac{h_y}{a_y(\gamma_y^{-1}(c^\ell))} \right)^2 + \left(\frac{h_z}{a_z(\gamma_z^{-1}(c^\ell))} \right)^2 = 1 \quad (12)$$

where $a_x(\gamma_x^{-1}(c^\ell))$, $a_y(\gamma_y^{-1}(c^\ell))$ and $a_z(\gamma_z^{-1}(c^\ell))$ are the distance ranges in the principle directions defined by the fitted directional variogram models, for each contribution bin, c^ℓ , where $\ell = 1, \dots, L$.

The variogram is inferred in off-diagonal directions by the following procedure; for all locations within the covariance table, the covariance value associated with the closest ellipsoid to the location is assigned. This is calculated quickly by solving Equation 12 for each ellipsoid proceeding from the smallest to the largest. The application of many bins results in a smooth interpolation of the off-diagonal variogram.

The application of nested ellipsoids for inferring the off-diagonal variogram is demonstrated for a 2-D example in Figure 9. The example 2-D covariance table was calculated from variogram models in the principal directions defined by flexible fit models. The variogram model in Figure 9 would not be possible with conventional variogram modeling techniques. Of course, there is no guarantee that the resulting variogram model in Figure 9 is positive definite. This will be dealt with in the next section.

Correct the Covariance Table for Positive Definiteness

The previously outlined method of applying constraints in the spectrum representation is applied to correct for positive definiteness. The practical steps include (1) translate the covariance table so that the origin is located at the table corners, (2) apply the discrete FFT to the table, (3) correct the spectrum by constraints 1 and 2 [Eq. (9)] and then (4) perform the inverse FFT and (5) translate the corrected covariance table origin back to the center of the table. These steps are demonstrated for the example covariance table (Figure 9) in Figure 10.

For the example covariance table the magnitude of correction is characterized by a plot of the difference between the original and the corrected covariance table and the histogram of the difference (Figure 11). Maximum change in this case is about 5% of the sill. The original and corrected variogram models are shown for the principal and two off-diagonal directions along with the corrected covariance table (Figure 12).

This method has some similarities to the methodology proposed by Yao and Journel (1998). The key difference is in the construction of the covariance tables. Our method focuses on the integration of geologic information through the flexible design of variogram models in the principal directions and the construction of a consistent covariance table. The Yao and Journel (1998) method automatically constructs the covariance table directly from the available sample data and then applies a preliminary smoothing to remove noise due to sparse data. The resulting smoothed covariance map is then corrected in spectrum for positive definiteness as outlined previously [Eq. (9)]. While this method streamlines the variogram modeling process, it may remove the opportunity to inject geologic information with respect to the heterogeneity and anisotropy and risks the possibility of over fitting noisy experimental data.

An Example of the Flexible Variogram Modeling Method

An example 2-D data set is shown in Figure 13. Variograms were calculated in the X and Y directions. The resulting variograms fitted by (1) traditional method of nested positive definite models and (2) flexible variogram modeling method as shown in Figure 14. The flexible variogram modeling method resulted in a positive definite variogram model that closely characterizes the directional experimental variograms.

There is no significant difference between the original and corrected variograms. The spectral corrected variogram model is better able to fit the experimental variogram. The corrected covariance table was applied to generate 10 sequential Gaussian simulation realizations and the resulting variograms are shown in Figure 15. Sequential Gaussian simulation is a common simulation algorithm that proceeds in Gaussian space and reproduces inputs statistics such as the histogram and variogram within statistical fluctuations. The variogram is reproduced within expected statistical fluctuations.

Conclusion

The choice of variogram model has a major affect on kriging and kriging-based simulation. These models have been limited to nested combinations of proven models. Geometric variogram models provide a suite of positive definite models for improved variogram modeling flexibility. Difficulties still remain in utilizing these geometric models due to the intractable inverse problem of assessing the geometric object to match a required continuity structure; however, knowledge of a geologically based shape could provide a more reasonable basis to start modeling from.

Spectral corrected models offer an efficient methodology for improving variogram modeling. This technique allows variograms to be modeled with greater emphasis on geologic continuity information as opposed to limits imposed by the traditional method of nested structures. In practice the corrected variogram models are not so different from the uncorrected shapes. Many practitioners would like to fit directional variograms independently and then reconcile them in software. This provides a very practical solution.

The required computer code is straightforward and mostly available in the public domain. All variogram models proposed here are guaranteed to be positive definite; therefore, there are no issues with implementation. Fitting experimental variograms more closely leads to improved predictions. Numerous case studies are required to document this with sufficient backup.

References

Bochner, S., 1949, Fourier transform: Princeton Univ. Press, London, 219 p.

Deutsch, C.V. and Journel A.G., 1998, GSLIB: geostatistical software library and user's guide 2nd ed.: Oxford University Press, New York, 369 p.

Isaaks, E. H. and Srivastava R.M., 1989. An introduction to applied geostatistics: Oxford University Press, New York, 561 p.

Journel, A.G. and Huijbregts, Ch.J., 1978, Mining geostatistics: Academic Press, New York, 600 p.

Matérn, B., 1980, Spatial variation, volume 36 of lecture notes in statistics 2nd ed.: Springer-Verlag, New York, First edition published by Meddelanden fran Statens Skogsforskningsinstitut, band 49, no. 5, 1960, 151 p.

Miall, A. D., 1996, The geology of fluvial deposits: sedimentary facies, basin analysis and petroleum geology: Springer-Verlag Inc., Berlin, 582 p.

Press, W.H. et. al., 1992, Numerical recipes in FORTRAN 77 the art of scientific computing: Cambridge University Press Programs, 449 p.

Serra, J., 1967, Un critère nouveau de découvertes de structures: le variogramme: Sciences de la Terre, v. 12, p. 275-299.

Yao, T. and Journel A.G., 1998, Automatic modeling of (cross) covariance tables using fast Fourier transform: Math Geology, v. 30, no. 6, p. 589-615.

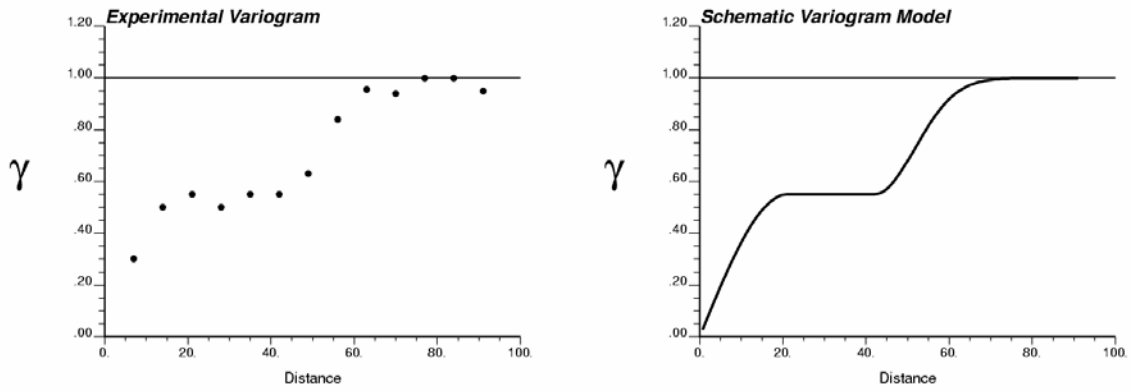


Figure 1 - An example variogram that is not well fit by nested sets of traditional variogram models.

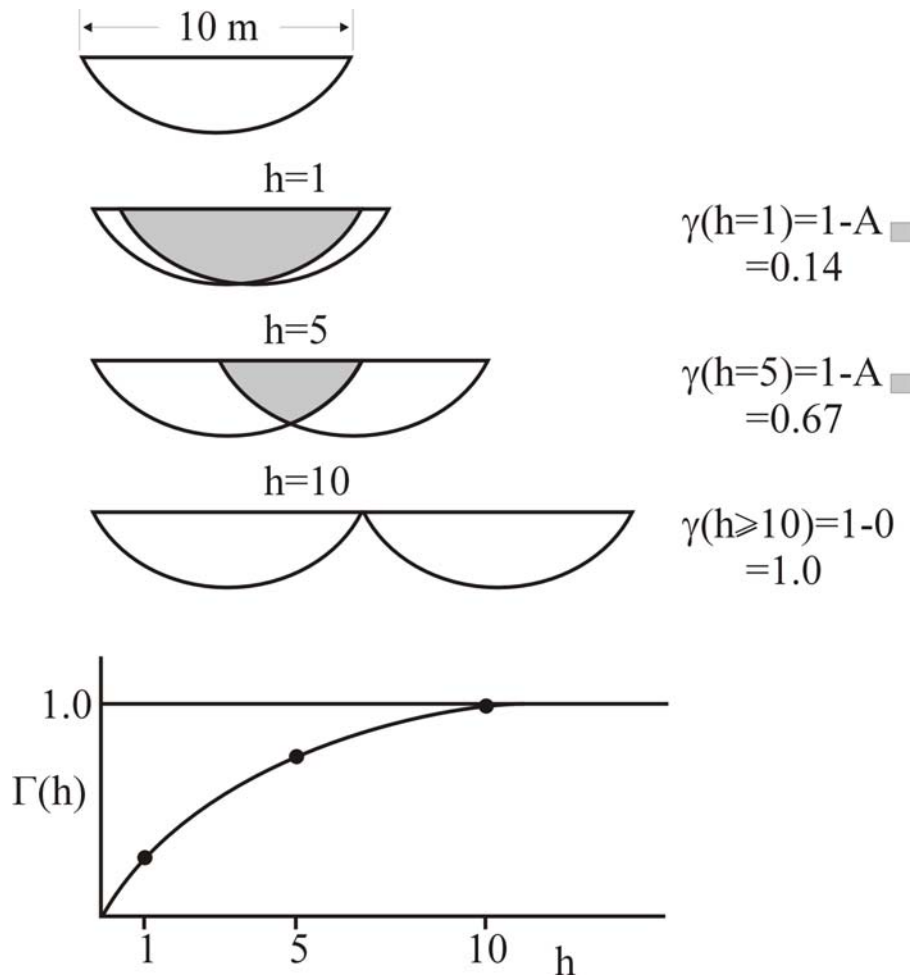


Figure 2 – An example geometric object and the resulting geometric variogram in the horizontal direction. Note that the variogram model will be anisotropic.

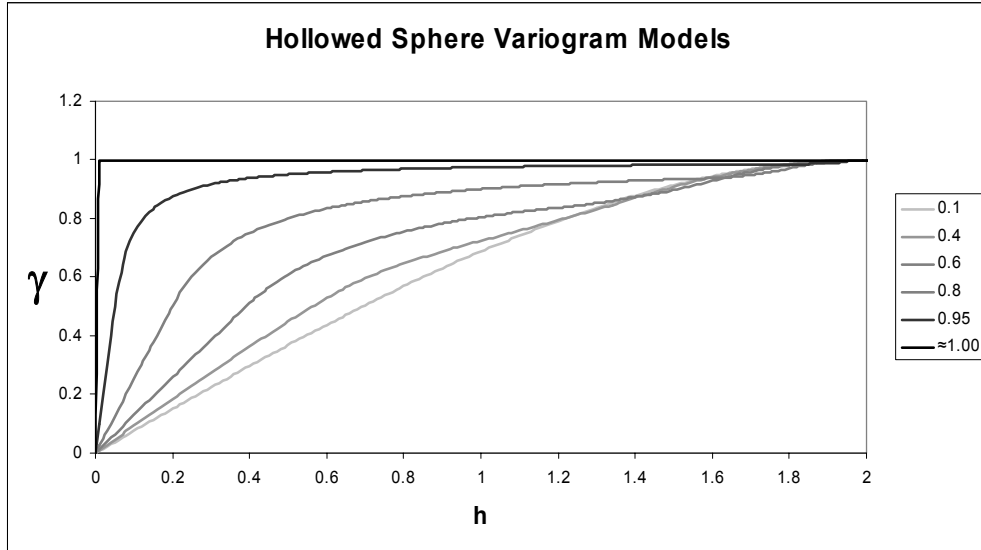


Figure 3 - A series of hollowed sphere variogram models. The sphere radius, r_2 , is set to 1.0 and the radius of the hollowing is varied.

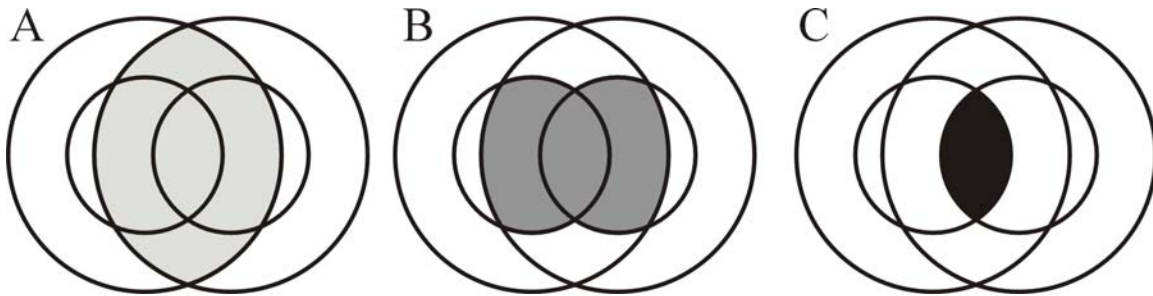


Figure 4 - Volumes v_1 , v_2 and v_3 (A, B and C): a traditional spherical variogram model is equal to standardized v_1 subtracted from the contribution. The hollowed sphere model is equal to the spherical minus v_2 plus v_3 .

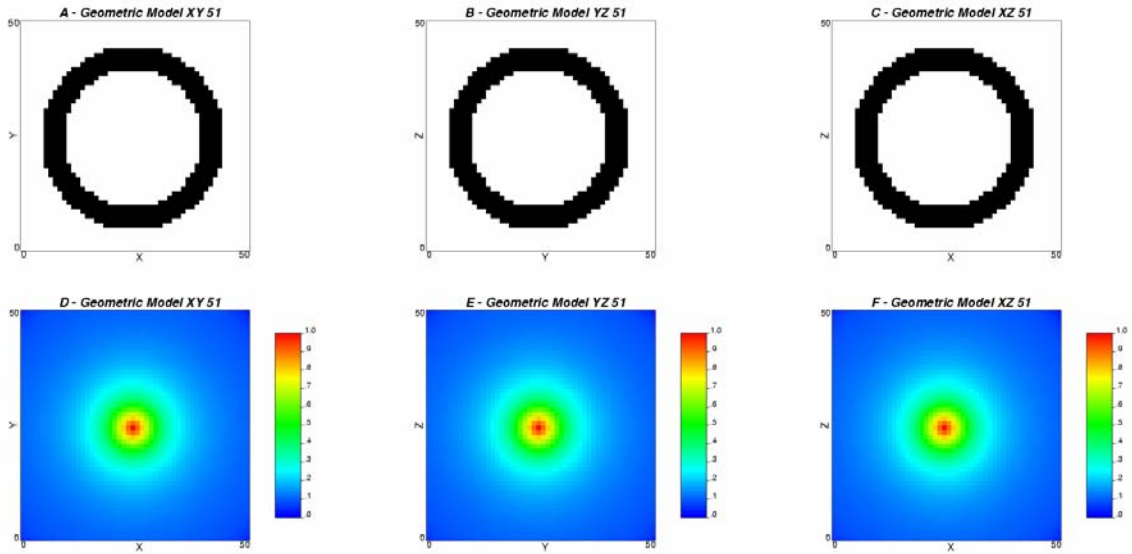


Figure 5 - Center slices through the rasterized geometric object and the resulting covariance table for the hollow spherical model with a hollowed fraction of 0.75.

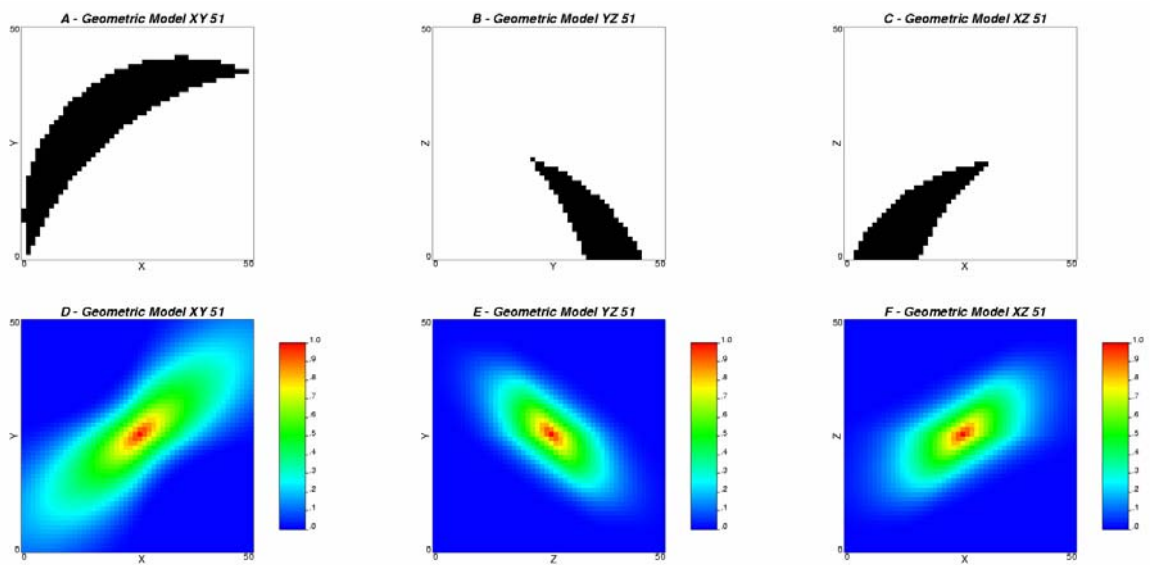


Figure 6 - Center slices through the raster geometric object and the resulting covariance table for a possible IHS point bar variogram.

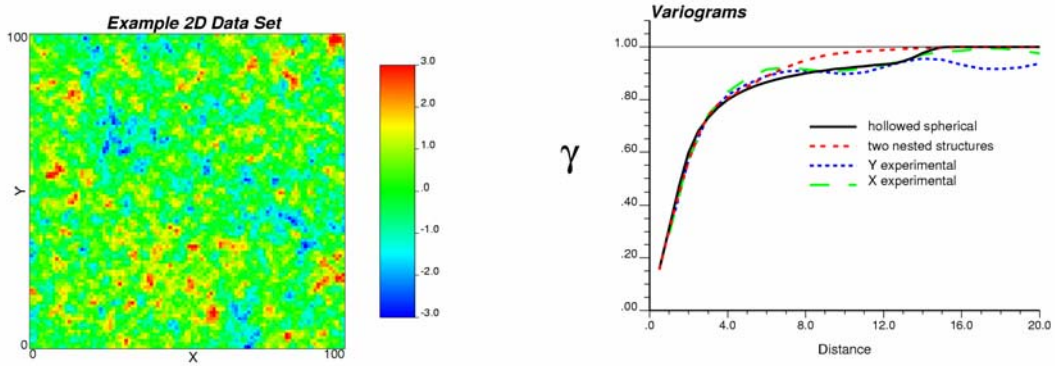


Figure 7 - The example 2D data set, the experimental variograms, a variogram model fitted with 2 nested spherical structures and a variogram model fitted with the hollowed spherical variogram model.

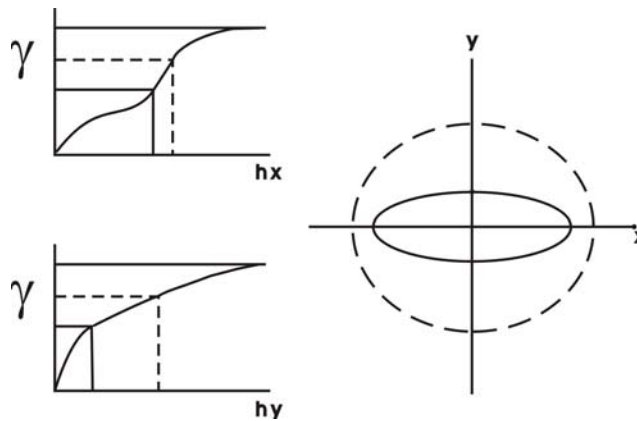


Figure 8 - Variable geometric anisotropy: the anisotropy ratios are allowed to vary with respect to variogram contribution. This results in the ability to consistently infer the variogram model in off-diagonal directions when the principal directions are not modeled by nested structures that exist in all directions. In this example the variogram is strongly anisotropic for the short range and then becomes more isotropic over the long range.

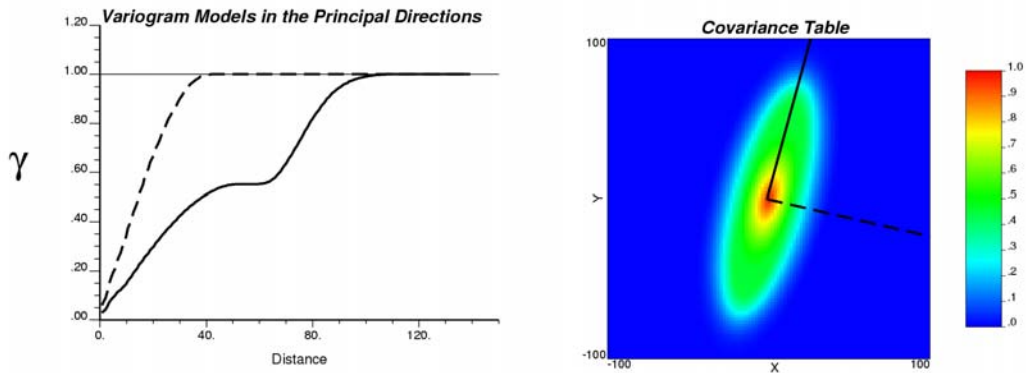


Figure 9 - The variogram models for the principal directions and the resulting covariance table. The covariance table is inferred with variable anisotropy.

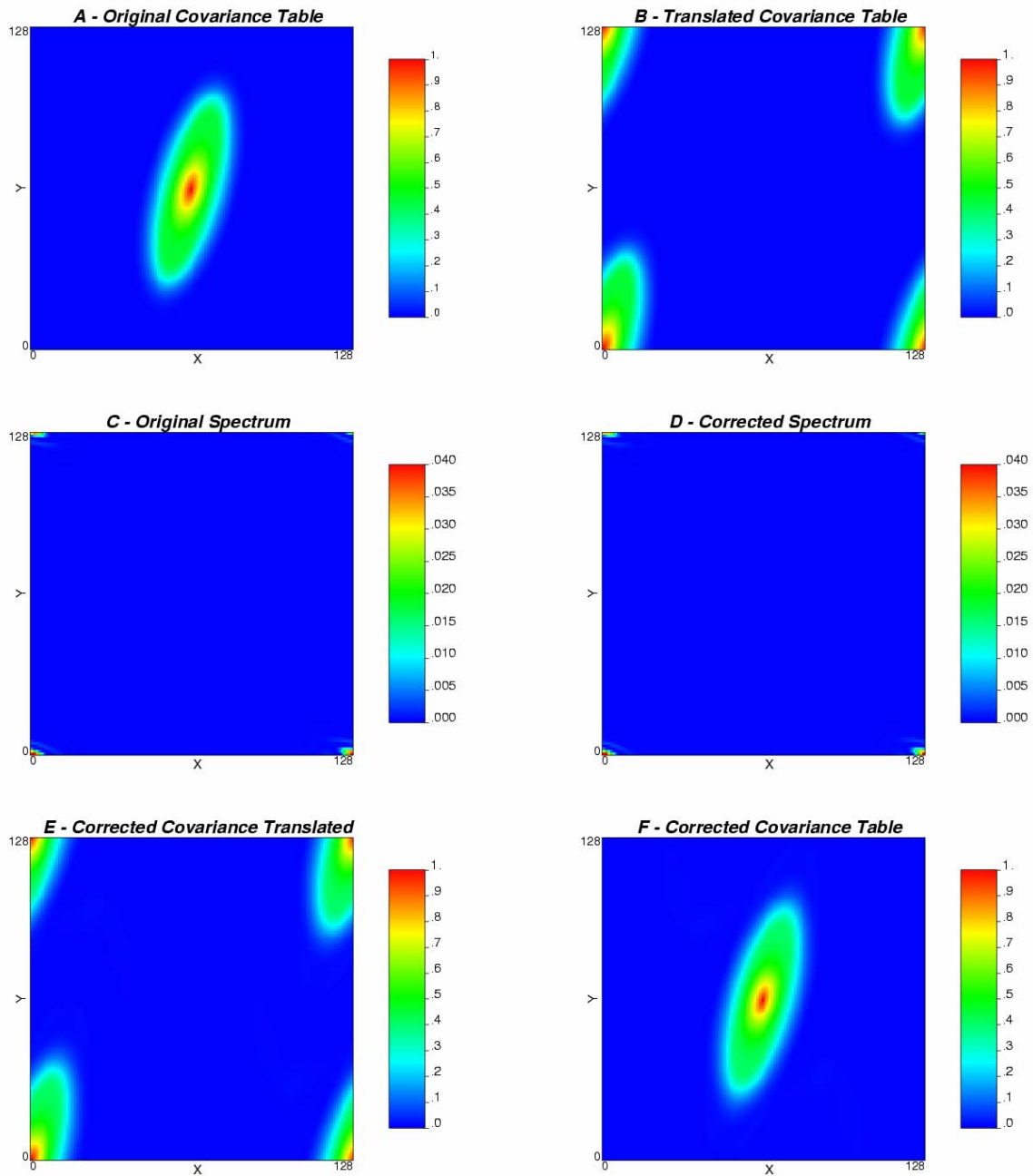


Figure 10 - The steps to correct the A, covariance table. (1) translate the covariance table so that the origin is located at the table corners, B, (2) apply the discrete FFT to the table, C , (3) correct the spectrum, D, and then (4) perform the inverse FFT, E, and (5) translate the corrected covariance table origin back to the center of the table, F.

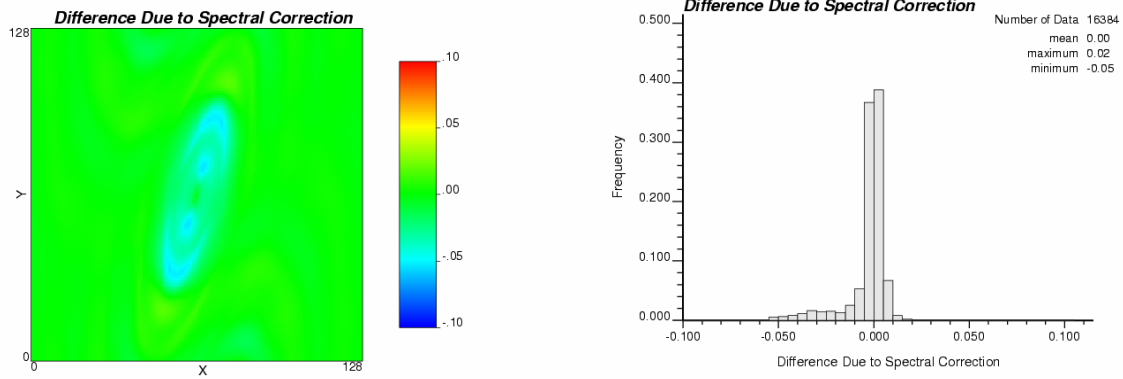


Figure 11 – The difference in the covariance table due to correction (corrected – original).

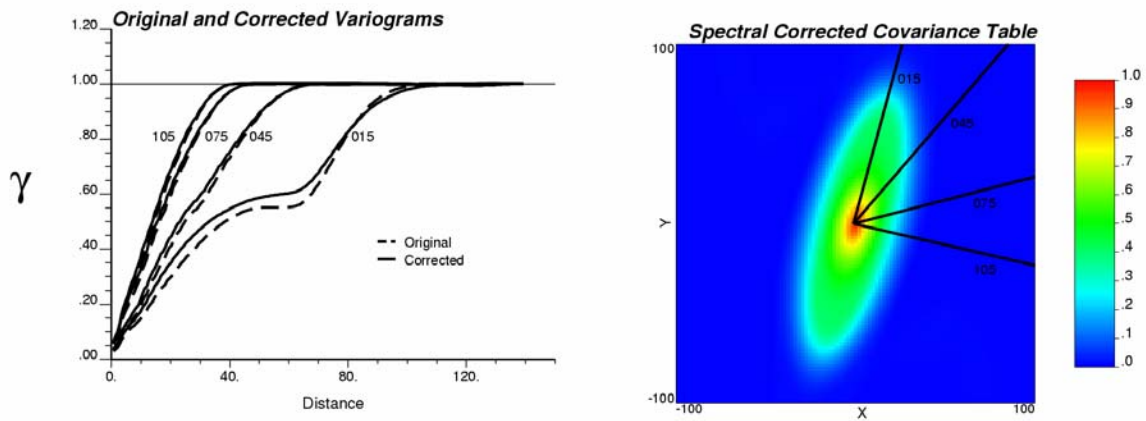


Figure 12 – A comparison of directional variograms from the original and corrected covariance tables.

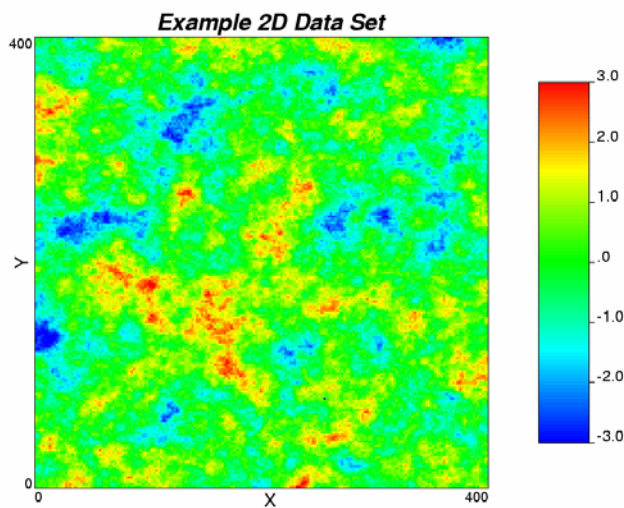


Figure 13 – An example 2D exhaustive data set.

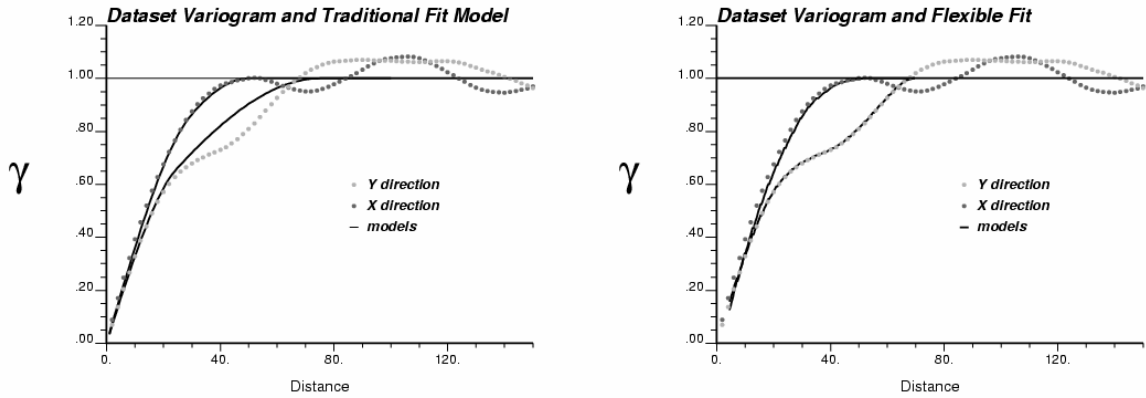


Figure 14 – The experimental variograms and the fit models based on the (1) traditional method of nested positive definite models and (2) flexible variogram modeling method. The variogram is modeled to the sill since the model will be applied in sequential Gaussian simulation.

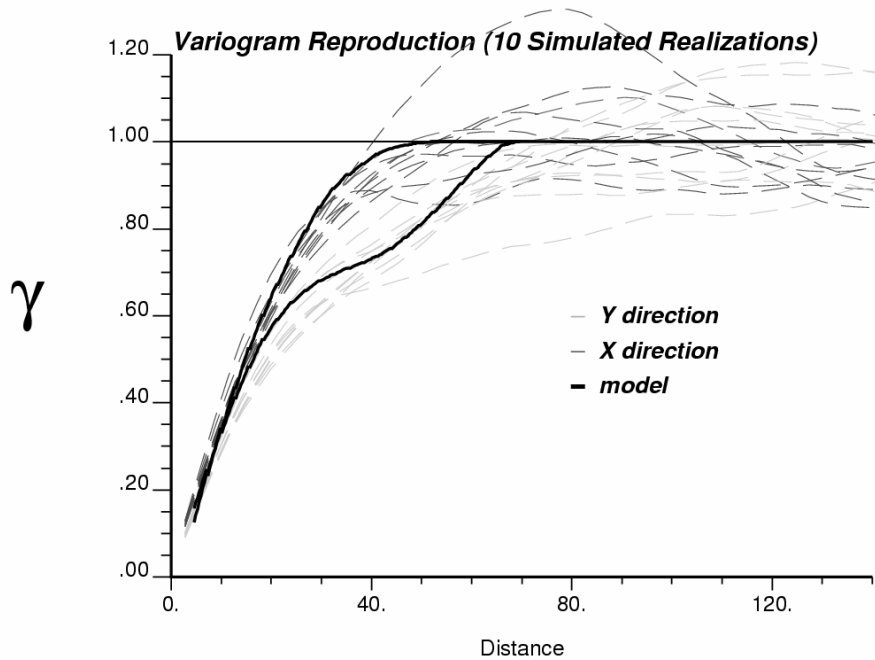


Figure 15 – The variogram model in the principal directions and the variograms calculated from 10 realizations. Over multiple realizations the important short range is closely reproduced. The significant inflection in the Y direction would not be reproduced with traditional variogram modeling.